AD-A063 076   DAVID W TAYLOR NAVAL SHIP RESEARCH AND DEVELOPMENT CE--ETC   F/G 17/8
DETERMINATION OF DISPLACEMENTS FROM HOLOGRAMS USING SIMPLY APPL--ETC(U)
DEC 78   J P SIKORA

UNCLASSIFIED   DTNSRDC-78/108   NL

1 OF 1

AD
A063076

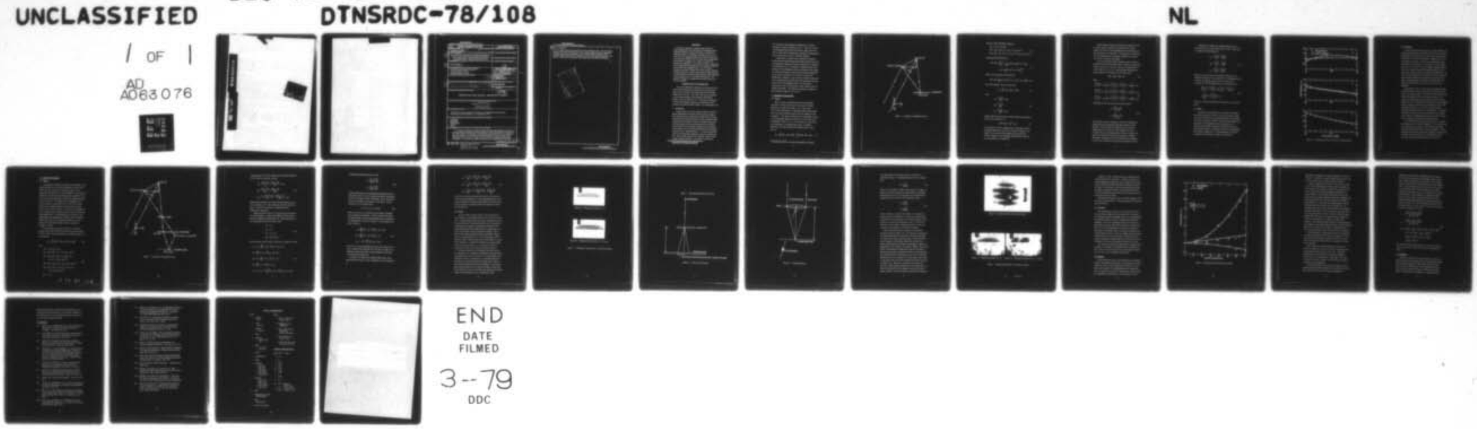

END
DATE
FILMED
3--79
DDC

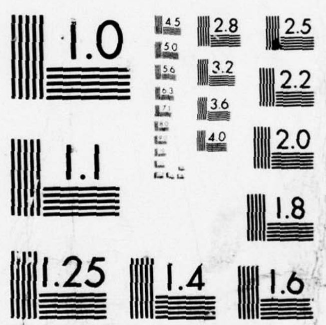

MICROCOPY RESOLUTION TEST CHART
NATIONAL BUREAU OF STANDARDS-1963-A

UNCLASSIFIED

SECURITY CLASSIFICATION OF THIS PAGE (When Data Entered)

14

REPORT DOCUMENTATION PAGE		READ INSTRUCTIONS BEFORE COMPLETING FORM
1. REPORT NUMBER DTNSRDC-78/108	2. GOVT ACCESSION NO.	3. RECIPIENT'S CATALOG NUMBER
4. TITLE (and Subtitle) 6 DETERMINATION OF DISPLACEMENTS FROM HOLOGRAMS USING SIMPLY APPLIED METHODS THAT ARE COMPARABLE TO SPECKLE TECHNIQUES.		5. TYPE OF REPORT & PERIOD COVERED 6. PERFORMING ORG. REPORT NUMBER
7. AUTHOR(s) 10 Jerome P. Sikora		8. CONTRACT OR GRANT NUMBER(s) 62543N 17
9. PERFORMING ORGANIZATION NAME AND ADDRESS David W. Taylor Naval Ship Research and Development Center Bethesda, Maryland 20084		10. PROGRAM ELEMENT, PROJECT, TASK AREA & WORK UNIT NUMBERS Block Program SF 43 422 593, Task Area ZR 023 01 01 Work Unit 1-1730-610 61152N
11. CONTROLLING OFFICE NAME AND ADDRESS 11		12. REPORT DATE December 1978 13. NUMBER OF PAGES 28
14. MONITORING AGENCY NAME & ADDRESS (if different from Controlling Office) 9 Research and development rept.,		15. SECURITY CLASS. (of this report) UNCLASSIFIED 15a. DECLASSIFICATION/DOWNGRADING SCHEDULE

16. DISTRIBUTION STATEMENT (of this Report)

12 30p.

APPROVED FOR PUBLIC RELEASE: DISTRIBUTION UNLIMITED

17. DISTRIBUTION STATEMENT (of the abstract entered in Block 20, if different from Report)

16 F43422, ZR02301

18. SUPPLEMENTARY NOTES

Presented at the 6th International Conference for Experimental Stress Analysis, held in Munich, West Germany, 18–22 September 1978.

19. KEY WORDS (Continue on reverse side if necessary and identify by block number)

Holography
Image-Plane
Displacements
Speckle

20. ABSTRACT (Continue on reverse side if necessary and identify by block number)

A system of equations is developed which relates the general displacement field from usual and image-plane double exposure holograms of objects illuminated by collimated or point light sources. By defining a coordinate system in the direction of the holographic plate and requiring that the object be several plate diameters from the plate, certain simplifications in the system of equations can be made to decouple the displacement components. As a result, the in-plane components can be independently determined → next page

(Continued on reverse side)

DD FORM 1 JAN 73 1473 EDITION OF 1 NOV 65 IS OBSOLETE
S/N 0102-014-6601

UNCLASSIFIED

SECURITY CLASSIFICATION OF THIS PAGE (When Data Entered)

387682

LB

(Block 20 continued)

from the apparent fringe shift observed from the holographic plate. The out-of-plane component can then be solved from a linear equation using the in-plane components. All three components of displacement can be simultaneously determined from a single film plate, regardless of the proportion of in- to out-of-plane components. The method is validated by comparisons with speckle results and theoretical analyses.

ABSTRACT

A system of equations is developed which relates the general displacement field from usual and image-plane double exposure holograms of objects illuminated by collimated or point light sources. By defining a coordinate system in the direction of the holographic plate and requiring that the object be several plate diameters from the plate, certain simplifications in the system of equations can be made to decouple the displacement components. As a result, the in-plane components can be independently determined from the apparent fringe shift observed from the holographic plate. The out-of-plane component can then be solved from a linear equation using the in-plane components. All three components of displacement can be simultaneously determined from a single film plate, regardless of the proportion of in- to out-of-plane components. The method is validated by comparisons with speckle results and theoretical analyses.

ADMINISTRATIVE INFORMATION

The work summarized in this report was sponsored in part by the Naval Sea Systems Command (03511) from elements which are now included in the Surface Ship Structures Block Program SF 43 422 593. Part of the work was also sponsored by the In-House Research and Exploratory Development Program, Task Area ZR 023 01 01. This report was presented at the 6th International Conference for Experimental Stress Analysis held in Munich, West Germany, 18–22 September 1978.

1. Introduction

Several authors [1–6] have proposed methods to derive the general displacement field from a double exposure hologram. The methods have been cumbersome to apply because they have relied upon measuring fringe locations in space, knowing detailed coordinates on the surface of an object, or taking a large number of fringe readings to solve over-determined sets of equations. Other methods, which are simpler to apply, have been proposed for such special cases as out-of-plane deformations, pure bending, simple shapes, etc. Additional work [7–11] has been expended in the use of image-plane holograms to measure a displacement field. These methods also tend to be awkward to apply, require complex imaging techniques, or be limited to special cases.

The advantages, disadvantages, and limitations of speckle[1]) techniques are well documented [12–17]. There is an interest in developing methods which are simple to apply and can be used to obtain all three displacement components simultaneously from a general object subject to arbitrary loadings.

In this paper, a system of three equations is developed which relates the general displacement field obtained from usual and image-plane holograms of objects illuminated by collimated or point light sources. By defining a coordinate system in the directions of the holographic plate and requiring that the object be several plate diameters from the plate, certain simplifications in the system of equations can be made to decouple the displacement components. As a result, the in-plane components can be independently determined from the apparent fringe shift observed from the holographic plate. The out-of-plane component can then be solved from a linear equation with the in-plane components. The method of analysis is analogous to that reported in references [5] and [9].

2. Holographic Interferometry

2.1 Theory

When an object is displaced between two holographic exposures, the fringes which appear are related to constant differences of optical path length. Let an object point $P(X, Y, Z)$ be illuminated by a collimated object beam parallel to the X-Z plane, making an angle α with the negative Z axis; see Figure 1. The object is observed from a point $H(X_k, Y_k, Z_k)$ on the holographic film plate, which is in an X-Y plane. Let P be displaced to $P'(X + U, Y + V, Z + W)$ where U, V, and W are the components of the displacement vector. The phase difference of the light arriving at H through P and P′ can be given by

$$\delta_k = \frac{2\pi}{\lambda} [P'H - (AP + PH)] = \frac{2\pi}{\lambda} [(P'H - PH) - AP] \qquad (1)$$

[1]) All subsequent references to speckle assume single-beam techniques.

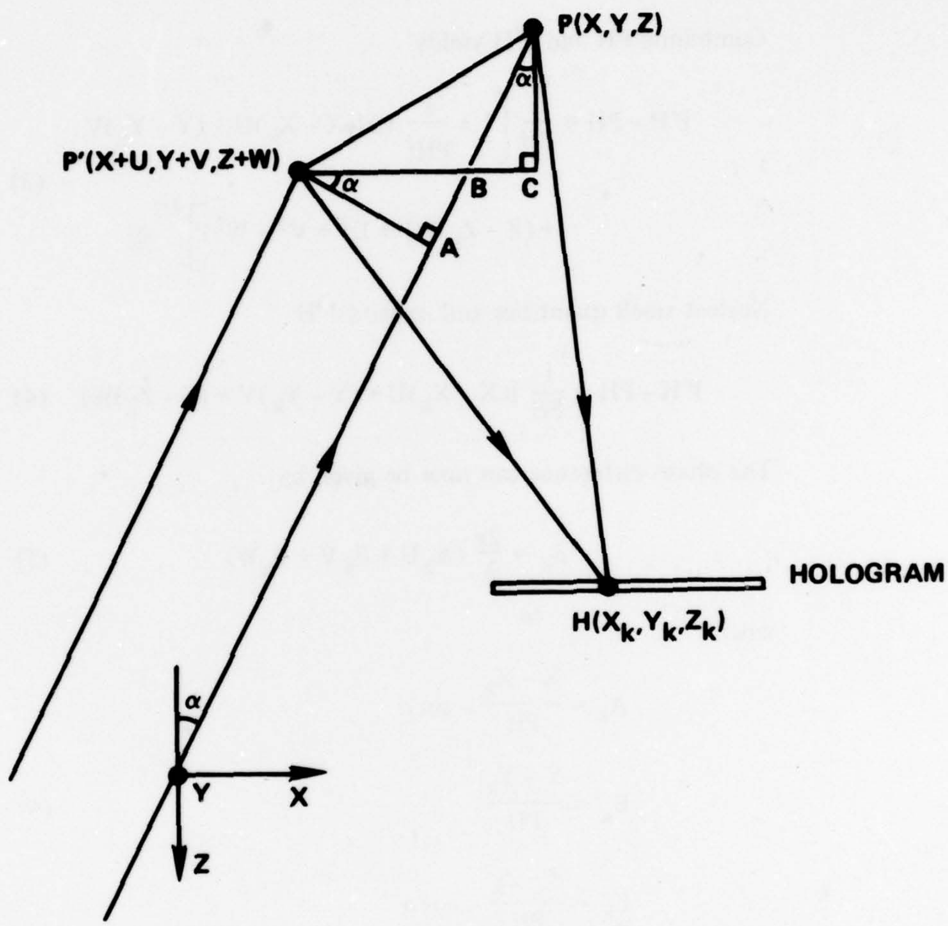

Figure 1 – Schematic of Holographic Setup

where λ is the wavelength of light and

$$\begin{aligned} AP &= U \sin\alpha + W \cos\alpha \\ PH &= [(X - X_k)^2 + (Y - Y_k)^2 + (Z - Z_k)^2]^{1/2} \qquad (2) \\ P'H &= [(X - X_k + U)^2 + (Y - Y_k + V)^2 + (Z - Z_k + W)^2]^{1/2} \end{aligned}$$

Combining PH and P'H yields

$$P'H - PH = \frac{1}{PH}\left[1 + \frac{1}{PH^2}(2[(X - X_k)U + (Y - Y_k)V + (Z - Z_k)W] + U^2 + V^2 + W^2)\right]^{1/2} \qquad (3)$$

Neglect small quantities and expand P'H

$$P'H - PH = \frac{1}{PH}[(X - X_k)U + (Y - Y_k)V + (Z - Z_k)W] \qquad (4)$$

The phase difference can now be given by

$$\delta_k = \frac{2\pi}{\lambda}(A_k U + B_k V + C_k W) \qquad (5)$$

where

$$\begin{aligned} A_k &= \frac{X - X_k}{PH} - \sin\alpha \\ B_k &= \frac{Y - Y_k}{PH} \qquad (6) \\ C_k &= \frac{Z - Z_k}{PH} - \cos\alpha \end{aligned}$$

Bright fringes will occur when the phase difference δ_k (equation (5)) is an even multiple of π

$$A_k U + B_k V + C_k W = n_k \lambda \qquad (7)$$

The subscript k refers to a single point of observation from the holographic film plate, and n_k is the number of fringes on the image. The same point on the image can be viewed from different locations on the film plate, giving different values for n_k, and appearing as a fringe shift.

Three observation points will yield three equations of type (7) which, ideally, is sufficient to determine U, V, and W. However, the value of the determinant can be small because of the limited size of the film plate. The least-squares combination of an overdetermined set of equations suggested in references [5] and [6] overcomes this problem.

Let us now introduce some restrictions upon a system of equations from three observation points. Choose the observation points so that $Y_2 = Y_1$ and $X_3 = X_1$; since the film plate is in an X-Y plane, $Z_1 = Z_2 = Z_3$. If the film plate dimensions are small compared to its distance from the object, then

$$PH_1 \doteq PH_2 \doteq PH_3 = R \tag{8}$$

Hence

$$\begin{aligned}
&\left(\frac{X - X_1}{R} - \sin\alpha\right)U + \left(\frac{Y - Y_1}{R}\right)V + \left(\frac{Z - Z_1}{R} - \cos\alpha\right)W = n_1\lambda \\
&\left(\frac{X - X_2}{R} - \sin\alpha\right)U + \left(\frac{Y - Y_1}{R}\right)V + \left(\frac{Z - Z_1}{R} - \cos\alpha\right)W = n_2\lambda \\
&\left(\frac{X - X_1}{R} - \sin\alpha\right)U + \left(\frac{Y - Y_3}{R}\right)V + \left(\frac{Z - Z_1}{R} - \cos\alpha\right)W = n_3\lambda
\end{aligned} \tag{9}$$

Combining the first with second and third equations

$$\begin{aligned}
U &= \frac{R\lambda(n_1 - n_2)}{X_2 - X_1} \\
V &= \frac{R\lambda(n_1 - n_3)}{Y_3 - Y_1}
\end{aligned} \tag{10}$$

The in-plane U- and V-components can now be independently determined from the apparent fringe shift observed in each direction. The out-of-plane W-component can be found by substituting U and V into one of the equations of set (9). Equation (10) is conceptually similar to those of reference [2], where the projections of all three components are similarily determined. Equations (9) and (10) maximize the projections of two of the components and separately determine the third.

Reference [5] replaces the collimated light source by a point light source, located at point $S(X_o, Y_o, Z_o)$. This results in equation (6) being replaced by

$$A_k = \frac{X - X_o}{SP} + \frac{X - X_k}{PH}$$

$$B_k = \frac{Y - Y_o}{SP} + \frac{Y - Y_k}{PH} \tag{11}$$

$$C_k = \frac{Z - Z_o}{SP} + \frac{Z - Z_k}{PH}$$

Using the same restrictions as described previously, we can substitute equation (11) into equation (9). Combining equations as before, we duplicate equation (10) for the U- and V-components. The W-displacement can be determined from

$$\left(\frac{X - X_o}{R_o} + \frac{X - X_1}{R}\right)U + \left(\frac{Y - Y_o}{R_o} + \frac{Y - Y_1}{R}\right)V$$
$$+ \left(\frac{Z - Z_o}{R_o} + \frac{Z - Z_1}{R}\right)W = n_1 \lambda \tag{12}$$

where R_o = SP, the distance from the light source to the object point.

2.2 Results

An aluminum propeller blade (30-cm-diam) was loaded by a uniform air pressure of 219 Pa. The observed fringe readings from three locations on the resulting double exposure hologram were used in equations (10) and (12) to predict the displacement components. The displacement across the chord at the 70-percent blade radius were scaled to 6900 Pa (1.0 psi) and were plotted in Figure 2 along with those from an isoparametric finite element analysis [18]. The good agreement of all three components demonstrates the validity of the method.

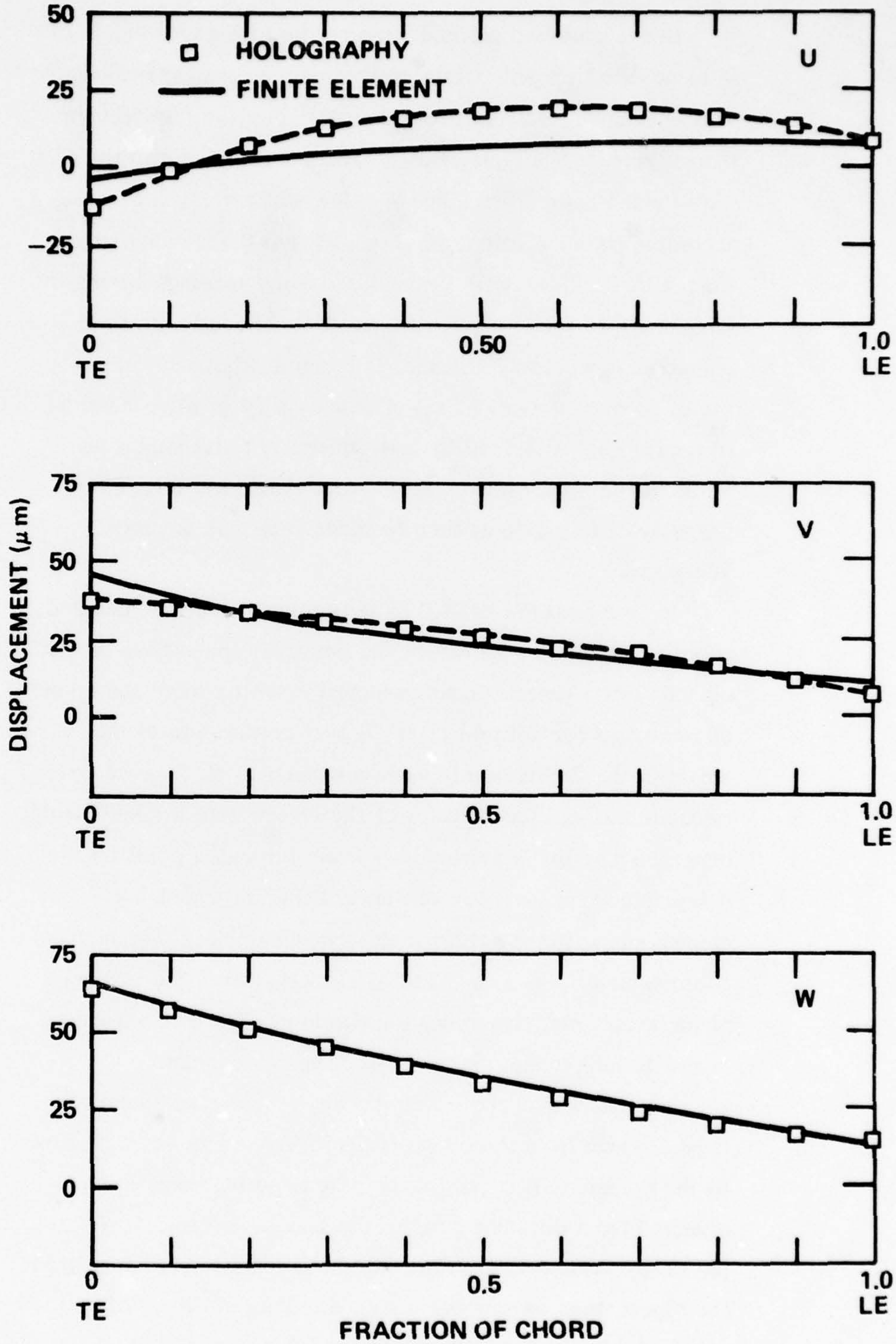

Figure 2 – Displacements across the Chord of Propeller Blade

2.3 Evaluation

In the proposed method, an error in a fringe reading in one in-plane direction produces a proportional error in the calculated displacement in that direction; the other in-plane displacement is unaffected. The same error produces a small error in the (W) out-of-plane component. The W value is affected less because, according to our restrictions, C of equation (7) is much larger than A or B. If we were to use three fringe readings, having the same error, to solve three equations simultaneously, all three components would be affected, sometimes catastrophically. The use of an over-determined set of equations (4 or more observed fringe readings combined by least-squares criteria) minimizes errors in the displacement calculations. Unfortunately, more fringe observations must then be made from one or more holograms.

In equations (9) or (12) of the proposed method, detailed coordinates must be known of the points on the surface of the object. For a general object, we must often resort to some kind of numerical control probe. If the surface variation of the object in the Z-direction is small compared to R, then we can calculate the X, Y coordinates of the object from the holographic image. By passing a narrow laser beam through a point on the holographic film plate, we can project the image and the corresponding fringe pattern onto a viewing plane. The in-plane coordinates of points can then be measured from the viewing plane, keeping any magnifications in mind. The errors involved in this technique are minimized as R becomes larger.

The restriction about keeping the hologram at a relatively large distance from the object is significant. If an object is close to the hologram, it is possible to have opposite fringe shifts observed from different parts of the same hologram. If we are physically prevented from moving the hologram far enough from the object, then one should use an overdetermined set of observed fringe values with equations (6), (7), and (11).

3. Image-Plane Holography

3.1 Theory

An image-plane hologram is formed when laser light from a collimated light source (as before) illuminates an object point $P(X, Y, Z)$ and is focused by a lens onto a point on the holographic film plate $I(X_i, Y_i, Z_i)$; see Figure 3. For simplicity, follow the scattered object ray which passes through the center of the lens, and let the image be focused on a film plate which is in an X-Y plane. If the object point is displaced for the second exposure to point $P'(X + U, Y + V, Z + W)$, it will be focused onto a slightly different X-Y plane than P at point $I'(X_i - mU, Y_i - mV, Z_i + m^2W)$. A reversal of the magnified U- and V- displacements is caused by the lens where m is its lateral image magnification. The W-displacement is affected by the longitudinal image magnification, assumed equal to m squared. Points $H(X_k, Y_k, Z_k)$ are observation locations in a plane parallel to the film plate through which the image-plane hologram is viewed.

The total distance traveled by a light ray for the first exposure will be $(AP + PI + IH)$, while for the second exposure it is $(P'I' + I'H)$. The phase difference of the light arriving at H can be given by

$$\delta_k = \frac{2\pi}{\lambda} [(P'I' + I'H) - (AP + PI + IH)] \tag{13}$$

where

$$\begin{aligned}
AP &= U \sin\alpha + W \cos\alpha \\
PI &= [(X - X_i)^2 + (Y - Y_i)^2 + (Z - Z_i)^2]^{1/2} \\
P'I' &= [(X + MU - X_i)^2 + (Y + MV - Y_i)^2 \\
&\quad + (Z + (1 - m^2)W - Z_i)^2]^{1/2} \\
IH &= [(X_i - X_k)^2 + (Y_i - Y_k)^2 + (Z_i - Z_k)^2]^{1/2} \\
I'H &= [(X_i - mU - X_k)^2 + (Y_i - mV - Y_k)^2 \\
&\quad + (Z_i + m^2W - Z_k)^2]^{1/2} \\
M &= 1 + m
\end{aligned} \tag{14}$$

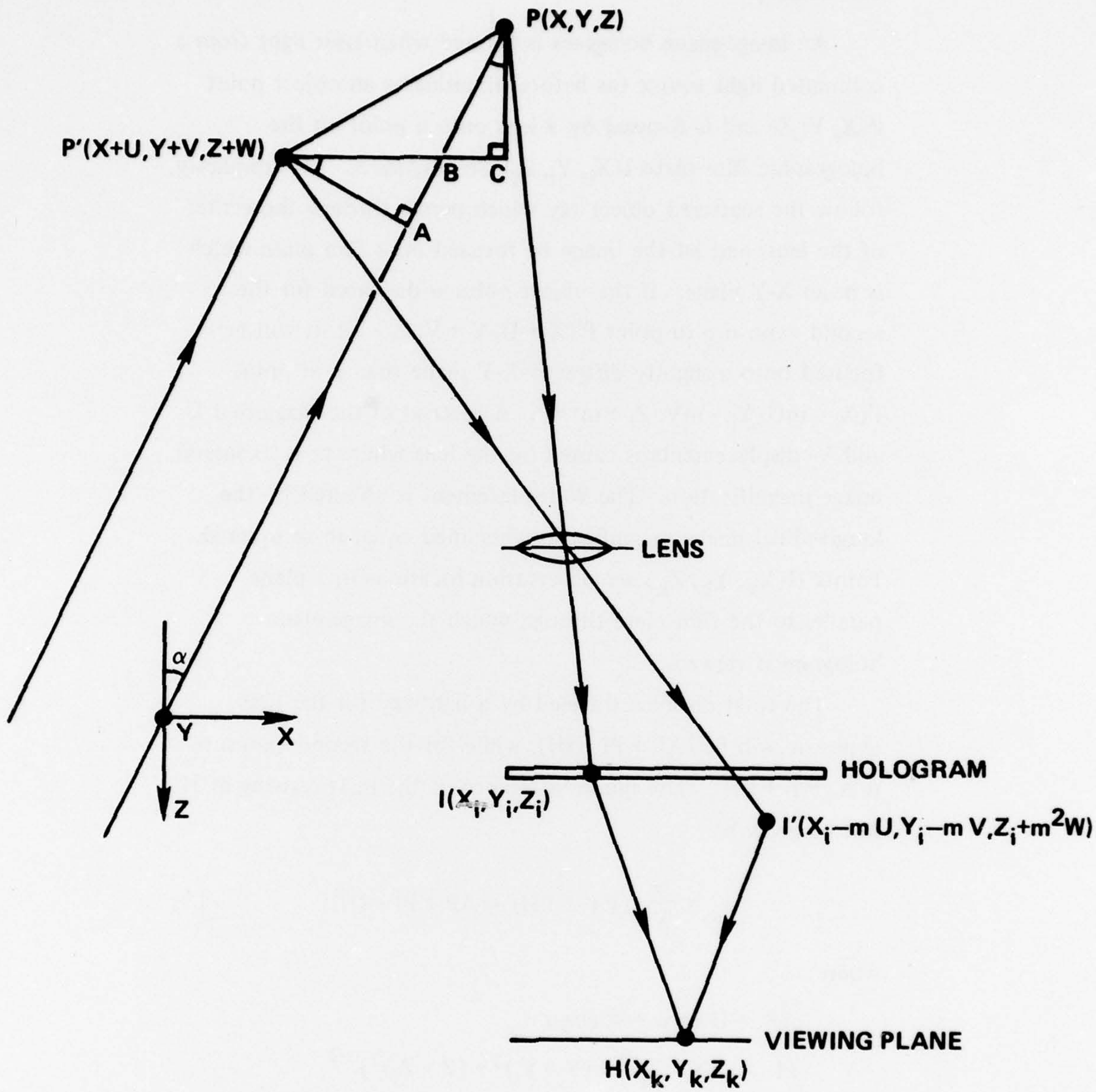

Figure 3 – Schematic of Image-Plane Setup

Combining P′I′ - PI and I′H - IH as before, the phase difference can be written by equation (5) where

$$A_k = \frac{M(X - X_i)}{PI} + \frac{m(X_k - X_i)}{IH} - \sin\alpha$$

$$B_k = \frac{M(Y - Y_i)}{PI} + \frac{m(Y_k - Y_i)}{IH} \tag{15}$$

$$C_k = \frac{(1 - m^2)(Z - Z_i)}{PI} - \frac{m^2(Z_k - Z_i)}{IH} - \cos\alpha$$

Bright fringes will again occur when the phase difference δ_k is an even multiple of π. Three observation points or, better yet, four or more will be necessary to determine the three displacement components.

Similar restrictions will now be introduced as was done for the usual holograms. A large focal length lens will be used to form the image-plane hologram, $PI_i \doteq R$. Observation points on the viewing plane should be chosen so that

$$\begin{aligned} Y_2 &= Y_1 \\ X_3 &= X_1 \\ Z_1 &= Z_2 = Z_3 \\ IH_1 &= IH_2 = IH_3 = r \end{aligned} \tag{16}$$

Three equations can be written in the form of equation (7) where

$$A_1 = A_3 = \frac{M}{R}(X - X_i) + \frac{m}{r}(X_1 - X_i) - \sin\alpha$$

$$A_2 = \frac{M}{R}(X - X_i) + \frac{m}{r}(X_2 - X_i) - \sin\alpha$$

$$B_1 = B_2 = \frac{M}{R}(Y - Y_i) + \frac{m}{r}(Y_1 - Y_i) \tag{17}$$

$$B_3 = \frac{M}{R}(Y - Y_i) + \frac{m}{r}(Y_3 - Y_i)$$

$$C_1 = C_2 = C_3 = \frac{(1 - m^2)}{R}(Z - Z_i) - \frac{m^2}{r}(Z_i - Z_1) - \cos\alpha$$

Combining equations as before, we have

$$U = \frac{(n_2 - n_1)\lambda r}{m(X_2 - X_1)}$$
$$V = \frac{(n_3 - n_1)\lambda r}{m(Y_3 - Y_1)} \tag{18}$$

In-plane displacements are independently determined from the fringe shift, and, they can be calculated without it being known where the film plate or object was located. We do not need to know the coordinates on the surface of the object. The W-component can be obtained from

$$W = (n_1\lambda - A_1 U - B_1 V)/C_1 \tag{19}$$

Since A_1, B_1, and C_1 are functions of the surface coordinates, more restrictions are required. If all the points on the object are approximately the same nominal distance from all points on the image IP(all i) = R, and $(Z - Z_i)/R \doteq 1$, then equation (17) can be written as

$$A_k = \frac{M^2}{mR}(X_L - X_i) + \frac{m}{r}(X_k - X_i) - \sin\alpha$$
$$B_k = \frac{M^2}{mR}(Y_L - Y_i) + \frac{m}{r}(Y_k - Y_i) \tag{20}$$
$$C_k = 1 - m^2 - \frac{m^2}{r}(Z_k - Z_i) - \cos\alpha$$

where X_L, Y_L is the longitudinal axis of the lens. Hence W, too, can be calculated from equation (19) with only the angle of the collimated object beam and the nominal distance of the object to the film plate being known.

Reference [9] replaces the collimated light source with a point light source $S(X_o, Y_o, Z_o)$. Equation (15) is now replaced by

$$A_k = \frac{X - X_o}{SP} + \frac{M(X - X_i)}{PI} + \frac{m(X_k - X_i)}{IH}$$

$$B_k = \frac{Y - Y_o}{SP} + \frac{M(Y - Y_i)}{PI} + \frac{m(Y_k - Y_i)}{IH} \tag{21}$$

$$C_k = \frac{Z - Z_o}{SP} + \frac{(1 - m^2)(Z - Z_i)}{PI} - \frac{m^2(Z_k - Z_i)}{IH}$$

With the same restrictions as before, U and V can be shown to be derived from equation (18). If the point light source can be placed sufficiently far from the object (SP all i = constant) then similar equations to equation (20) can be developed to predict the W-component.

3.2 Results

A steel cantilevered beam (240 by 12.6 by 2.8 mm) was point loaded in two orthogonal directions (Y and -Z) at the free end. A collimated light source was used to illuminate the beam from the fixed end 71 mm toward the free end. The image was recorded by a lens having a focal length of 190 mm at F4.5. Fringe readings from three locations on the viewing plane were made of the double exposure image-plane hologram. Photographs of the observed fringe pattern are presented in Figure 4 from two viewing locations (r = 1.2 m), 76 mm apart in the Y-direction. Only a slight variation in the fringe pattern was noted in the X-direction. A fringe shift (difference in fringe readings of the two viewing points) $n_3 - n_1$ of equation (18) of two fringes can be noted at the location indicated in Figure 4.

The image formed on the holographic film plate can also be considered to be a single-beam specklegram with slight optical noise produced by the reference beam. The specklegram can be evaluated by either a point-by-point or a full-field approach to determine the in-plane components of displacement. Figure 5 gives reconstruction methods of the specklegram. The point-by-point approach (Figure 5 (a)) consists of passing a narrow laser beam through a location on the image and observing the Young's fringes in the diffraction halo on a ground glass screen.

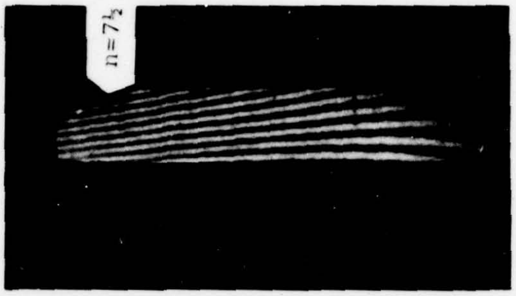

Figure 4a – Observed from Point X_1, Y_1

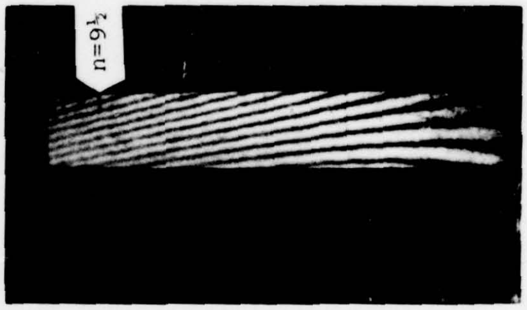

Figure 4b – Observed from Point X_1, Y_1 + 76 mm

Figure 4 – Holographic Fringe Pattern of Cantilevered Beam

Figure 5 – Specklegram Reconstruction Setup

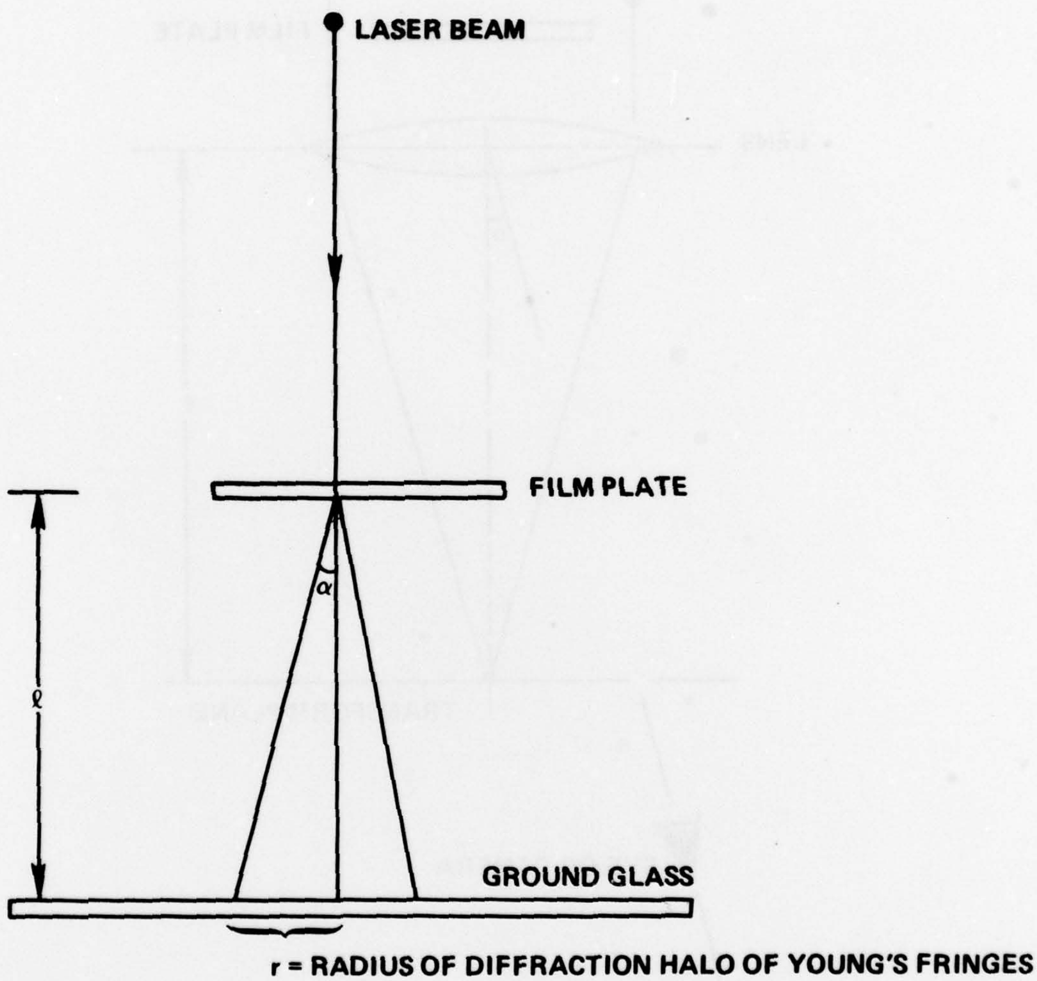

Figure 5a – Point-by-Point Method

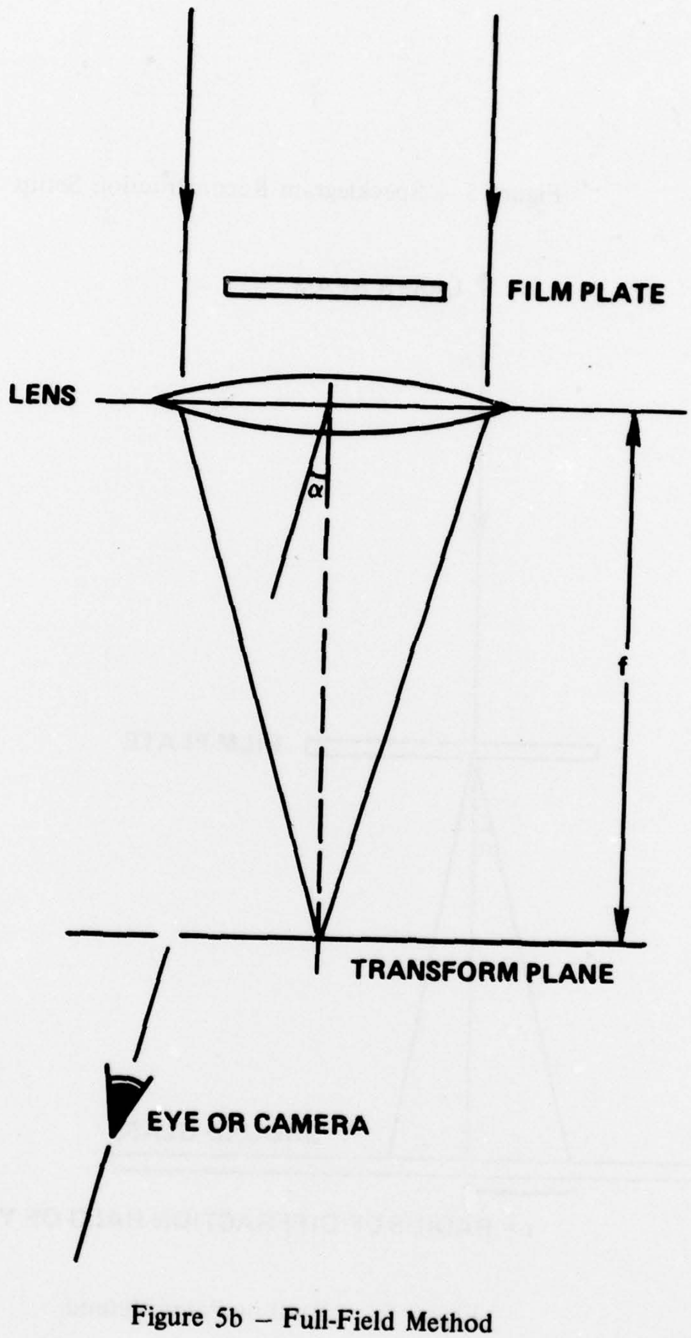

Figure 5b – Full-Field Method

The fringe pattern at the same location as in Figure 4 is presented in Figure 6. The displacements, D, can be evaluated from

$$D = \frac{n\lambda}{m \sin \alpha} \tag{22}$$

where n is the number of fringes which appear in an angle α of Figure 5 (a), and the direction is perpendicular to the fringes. Alternatively, the U- and V-components can be determined by using the sin α term in the X- and Y-directions, hence

$$U = \frac{n\lambda}{m \sin \alpha_x} \qquad V = \frac{n\lambda}{m \sin \alpha_y} \tag{23}$$

which is identical to equation (18) where n is the number of fringes passed moving between two points on the ground glass (equivalent to the viewing plane). The fringes of Figure 6 were produced by placing the ground glass screen 1.2 m from the film plate. If the number of fringes separated by 76 mm are counted in the Y-direction, two fringes are obtained.

Spatial filtering methods are required in the full-field approach depicted in Figure 5 (b). The film plate is illuminated in collimated laser light beyond which a lens focuses the light to a point on the focal or transform plane. If the film plate is viewed through a small aperture offset from the lens axis, a filtered image appears with fringes corresponding to contours of displacement in the direction of the offset. Figure 7 shows such fringes, corresponding to displacements near the V-direction, from aperture locations, separated by 76 mm in the Y-direction. The focal length of the transform lens was 1.2 m. The in-plane displacements can be calculated [17] from equation (23), where α is the angle of the axis of the transform lens and the aperture; see Figure 5 (b). Again this is equivalent to equation (18), where the transform plane corresponds to the viewing plane. As expected, a fringe shift of two fringes can be seen in the photographs of Figure 7 at the same location on the beam as in Figure 4.

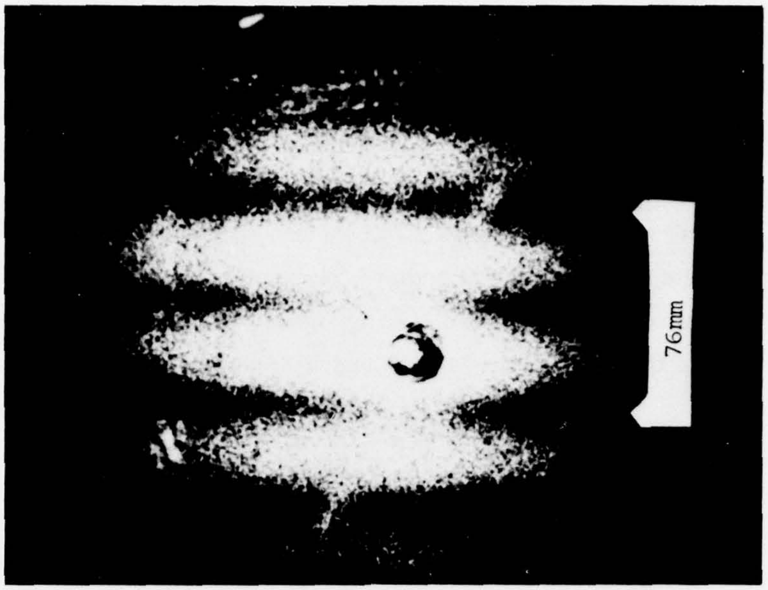

Figure 6 – Diffraction Halo with Young's Fringes

Figure 7a – Observed from Point X_1, Y_1 Figure 7b – Observed from Point X_1, Y_1 + 76 mm

Figure 7 – Speckle Fringe Pattern of Cantilevered Beam

Figures 4, 6, and 7 contain three sets of different fringe patterns from the same film plate. All three sets predict the same V-displacement component, can be analyzed by the same equation, and have the same fringe shift at a common location on the image. The solid angle in which the full-field speckle fringes are visible corresponds to the size of the diffraction halo in the point-by-point method and appears to limit the angle in which the image-plane fringes are visible.

Displacements along the beam are plotted in Figure 8 along with those from beam theory. The good agreement validates the proposed method.

3.3 Evaluation

The observations in section 2.3, concerning the effects of errors in fringe readings and overdetermined sets of equations, are valid for image-plane holograms as it was for usual holograms. An additional option is, however, available with image-plane holograms. One of the specklegram techniques can be used to determine the in-plane components and then use equations (19) with (17) or (20) to determine the out-of-plane components. Frequently it is physically easier to measure the spacings of the Young's fringes than it is to count the passage of a large number of fringes from two observation points. Alternatively, a least-squares combination of fringe shifts from two or all three of the techniques can be used with equations (5) with (17) or (20).

The restriction of keeping the film plate at a distance from the object is no problem if a relatively large focal length lens is used. Such a lens reduces the effects any out-of-plane components may have on the specklegram measurements.

4. Discussion

In determining the accuracy and sensitivity of the proposed methods consideration may be given to out-of-plane and in-plane conditions. When all of the displacement is limited to out-of-plane, and the angle of the collimated light source approaches zero, the fringes do not appear to shift position. Both the usual and image-plane equations reduce to the equation $W = n\lambda/2$.

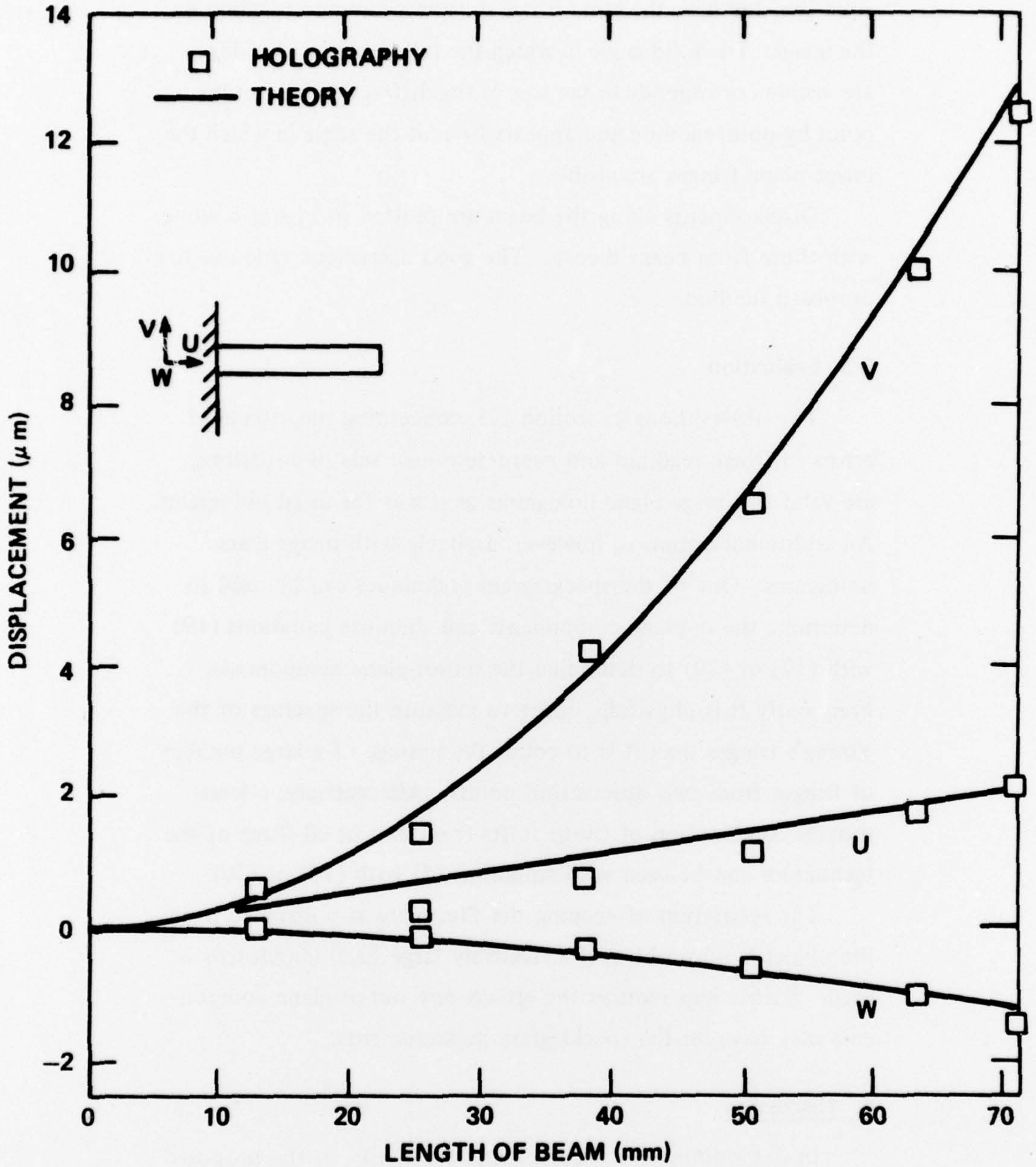

Figure 8 – Displacements along Cantilevered Beam

Uncertainty of an eighth of a fringe corresponds to an error of ± 30 nm ($\lambda = 488$ nm). If in-plane components are present, the error can increase with very large in-plane components.

Assume a magnification of unity, an F4.5 lens, and $r/\Delta X$ of 10 for the image-plane/specklegram in-plane measurements. An uncertainty of an eighth of a fringe shift corresponds to an error of ± 0.6 μm for the usual hologram, image-plane, and speckle methods. The minimum displacement which can be measured by the speckle techniques corresponds to slightly more than one fringe (two, full, dark half fringes in the diffraction halo) difference or 5 μm, which is in good agreement with the Rayleigh criteria for resolution based on speckle size. The minimum displacement which can be measured by the hologram techniques corresponds to that of the speckle techniques when all of the displacement is in-plane. However, when out-of-plane displacement is also present, a minimum in-plane displacement of 0.6 μm corresponding to an eighth of a fringe can be measured. The additional fringes provided by the W-displacement are analogous to the fringe mismatch method of Moirē techniques. Figure 4 is an example of the number of fringes which occur when the W-component is only 10 percent of the V-component.

Another approach to improving the accuracy and reducing the minimum displacements which can be measured is by using electronic phase measurement techniques, [19, 20] by which phase measurements corresponding to a thousandth of a fringe can be performed.

When a large out-of-plane displacement is present, the number of fringes may become so dense that the fringes cannot be distinguished because of the speckle noise. Image-plane holograms have an advantage over conventional holograms because they can be reconstructed in white light. As a result, the speckle noise can be reduced to the point where hundreds of fringes can be distinguished.

The proposed methods can be used to determine all three displacement components, regardless of their relative size or how they were formed. They do not require assumptions of elasticity to derive one type of displacement from another. Since all of the components can be measured from one film plate, nonlinear problems can be attempted. Often, primary concern is with strains and secondary concern is with displacements. For some simple cases, the surface strain of an object can be determined from the first derivative of the in-plane components, other simple cases can be satisfied by the second derivative of the normal component. A general curvilinear surface, however, requires the first derivatives of all three orthogonal displacement components to determine the surface strains. Reference [21] derives the following equations for a curvilinear surface in p and q, where X, Y, and Z as well as U, V, and W are functions of p and q.

$$
\begin{aligned}
\epsilon_p &= \frac{X_p U_p + Y_p V_p + Z_p W_p}{X_p^2 + Y_p^2 + Z_p^2} \\
\epsilon_q &= \frac{X_q U_q + Y_q V_q + Z_q W_q}{X_q^2 + Y_q^2 + Z_q^2} \\
\gamma_{pq} &= [X_p U_q + X_q U_p + Y_p V_q + Y_q V_p + Z_p W_q + Z_q W_p \\
&\quad - (\epsilon_p + \epsilon_q)(X_p X_q + Y_p Y_q + Z_p Z_q)] / \\
&\quad [(X_p Y_q - X_q Y_p)^2 + (Y_p Z_q - Y_q Z_p)^2 \\
&\quad + (Z_p X_q - Z_q X_p)^2]
\end{aligned}
\tag{24}
$$

The subscripts indicate differentiation. Of course, the geometry must be known of the surface of the object to determine the strains.

5. Conclusions

Systems of equations have been developed to quickly and easily determine the three displacement components from image-plane and regular holograms. The in-plane components are a function of the viewing location and the fringe shift, whereas the out-of-plane components require in addition the nominal distance of the object to the hologram. An advantage of the method is that all three components of displacement can be simultaneousely determined from one film plate, regardless of the proportion of in- to out-of-plane components, without the use of complex imaging techniques.

6. References

[1] Haines, K.A. and Hildebrand, B.P.: Surface Deformation Measurements Using the Wavefront Reconstruction Technique. Appl. Opt. 5(4) 1966.

[2] Aleksandrov, E.B. and Bonch-Bruevich, A.M.: Investigation of Surface Strains by the Hologram Technique. Soviet Phys., Tech. Phys. 12(2) 1967.

[3] Sollid, J.E.: Holographic Interferometry Applied to Measurements of Small Static Displacements of Difusely Reflecting Surfaces. Appl. Opt. 8(8) 1969.

[4] Abramson, N.: The Holo-Diagram: I. A Practical Device for Making and Evaluating Holograms; II. A Practical Device for Information Retrieval in Hologram Interferometry; III. A Practical Device for Predicting Fringe Patterns in Hologram Interferometry. Appl. Opt. 8(6) 1969, 9(1) 1970, 9(10) 1970.

[5] Dhir, S.K. and Sikora, J.P.: An Improved Method for Obtaining the General-Displacement Field from a Holographic Interferogram. Exp. Mech. 12(7) 1972.

[6] King, P.W. III: Holographic Interferometry Technique Utilizing Two Plates and Relative Fringe Orders for Measuring Micro-Displacements. Appl. Opt. 13(2) 1974.

[7] Brandt, G.B.: Image Plane Holography. Appl. Opt. 8(7) 1969.

[8] Adams, F.D. and Maddux, G.E.: Synthesis of Holography and Speckle Photography to Measure 3-D Displacements. Appl. Opt. 13(2) 1974.

[9] Sikora, J.P.: A Three-Dimensional Displacement Analysis from an Image-Plane Hologram. presented at 1977 SESA Spring Meeting, Dallas, Texas, to be published in Exp. Mech.

[10] Exner, G.A. and Gilbert, J.A.: Displacement Analysis Using Image-Plane Holography. presented at 1977 SESA Spring Meeting, Dallas, Texas.

[11] Gilbert, J.A. and Exner, G.A.: An Image-Plane Technique to Separate Components of Displacement by Optical Filtering of Holographic-Moiré Patterns. presented at 1977 SESA Spring Meeting, Dallas, Texas.

[12] Leendertz, J.A.: Interferometric Displacement Measurement on Scattering Surfaces Utilising Speckle Effect. J. Phys. E. Sci. Inst., Vol. 3, 1970.

[13] Archbold, E., Burch, J., and Ennos, A.: Recording of In-Plane Surface Displacements by Double Exposure Speckle Photography. Opt. Acta, 17, 1970.

[14] Adams, F.D. and Maddux, G.E.: On Speckle Diffraction Interferometry for Measuring Whole Field Displacements and Strains. Air Force Flight Dynamics Lab., Tech. Report 72-123, 1973.

[15] Cloud, G.: Practical Speckle Interferometry for Measuring In-Plane Deformation. Appl. Opt. 14(4) 1975.

[16] Khetan, P. and Chiang, F.P.: Strain Analysis by One-Beam Laser Speckle Interferometry - Single Aperature Method. Appl. Opt. 15(9) 1976.

[17] Barker, D.B. and Fourney, M.E.: Displacement Measurement in the Interior of 3-D Bodies Using Scattered Light Speckle Patterns. Exp. Mech. 16(6) 1976.

[18] Ma, J.H.: Stresses in Marine Propellers. J. Ship Research 18(4) 1974.

[19] Dändiker, R., Ineichen, B., and Mottier, F.: High Resolution Hologram Interferometry by Electronic Phase Measurement. Opt. Comm. 9(4) 1973.

[20] Dändiker, R., Ineichen, B., and Mottier, F.: Electronic Processing of Holographic Interferograms. presented at the 1974 Int. Opt. Computing Conf., Zurich, Switzerland.

[21] Dhir, S.K. and Sikora, J.P.: Holographic Determination of Surface Stresses in an Arbitrary Three-Dimensional Object. presented at the 1974 Int. Opt. Computing Conf., Zurich, Switzerland.

INITIAL DISTRIBUTION

Copies	
1	DDR&E Lib
1	CNO OP 098T
1	CHONR Code 474
1	DNL
2	NAVMAT 1 MAT 08T23 1 Lib
2	NRL 1 Code 8431 1 Tech Lib
1	USNA
1	NAVPGSCOL
1	NOSC
6	NAVSEA 1 SEA 03 1 SEA 03C 1 SEA 035 1 SEA 03511 1 SEA 03522 1 SEA 09G32
5	NAVSEC 1 SEC 6110 1 SEC 6113 1 SEC 6114D 1 SEC 6120D 1 SEC 6128
12	DDC
1	Wright-Patterson AFT AFFDL-FBEC
1	NSF Engr Div Lib
1	Library of Congress
1	Univ. of Connecticut Dept. of M.E.
2	Michigan St. Univ. MMM Dept.
1	Univ. of Wisconsin at Milwaukee Dept. of Mechanics
1	Beta Industries, Inc. Dayton, Ohio
1	United Tech. Res. Cntr. Instrumentation Lab.

CENTER DISTRIBUTION

Copies	Code	Name
1	012	
1	17	
1	1702	
1	1706	
1	1720	
10	1730	
1	1740	
1	1770	
1	1844	
1	274	
10	5214.1	Reports Distribution
1	522.1	Unclass Lib (C)
1	522.2	Unclass Lib (A)